The *Neisseria meningitidis* CRISPR-Cas9 System Enables Specific Genome Editing in Mammalian Cells

Ciaran M Lee[1], Thomas J Cradick[2,3] and Gang Bao[1]

[1]Department of Bioengineering, Rice University, Houston, Texas, USA; [2]Department of Biomedical Engineering, Georgia Institute of Technology and Emory University, Atlanta, Georgia, USA; [3]Present Address: CRISPR Therapeutics, Cambridge, Massachusetts, USA

The clustered regularly-interspaced short palindromic repeats (CRISPR)—CRISPR-associated (Cas) system from *Streptococcus pyogenes (Spy)* has been successfully adapted for RNA-guided genome editing in a wide range of organisms. However, numerous reports have indicated that *Spy* CRISPR-Cas9 systems may have significant off-target cleavage of genomic DNA sequences differing from the intended on-target site. Here, we report the performance of the *Neisseria meningitidis* (*Nme*) CRISPR-Cas9 system that requires a longer protospacer-adjacent motif for site-specific cleavage, and present a comparison between the *Spy* and *Nme* CRISPR-Cas9 systems targeting the same protospacer sequence. The results with the native crRNA and tracrRNA as well as a chimeric single guide RNA for the *Nme* CRISPR-Cas9 system were also compared. Our results suggest that, compared with the *Spy* system, the *Nme* CRISPR-Cas9 system has similar or lower on-target cleavage activity but a reduced overall off-target effect on a genomic level when sites containing three or fewer mismatches are considered. Thus, the *Nme* CRISPR-Cas9 system may represent a safer alternative for precision genome engineering applications.

INTRODUCTION

Clustered, regularly-interspaced short palindromic repeats (CRISPR) and CRIPSR-associated (Cas) proteins constitute an acquired immune system in bacteria and archaea.[1] The type II CRISPR-Cas9 system from *Streptococcus pyogenes (Spy)* has been adapted to target distinct genomic loci in a wide variety of organisms.[2–9] This system is composed of a Cas9 protein, a trans-activating CRISPR RNA (tracrRNA), and a targeting CRISPR RNA (crRNA) that can be programmed to recognize a genomic sequence via Watson-Crick base pairing.[10] Furthermore, the tracrRNA and crRNA (2-RNA system) can be fused to create a single guide RNA (sgRNA).[10] Unlike other genome-editing tools such as zinc finger nucleases (ZFNs)[11] and transcription activator-like effector nucleases (TALENs)[12] that require engineered protein domains to target specific DNA sequences, in a CRISPR-Cas9 system the binding of endonuclease (Cas9) to

DNA is guided by a short RNA. The targeting region of a crRNA (2-RNA system) or a sgRNA (single guide system) will herein be referred to as the guide RNA (gRNA). DNA-targeting specificity is determined by two key factors: a DNA sequence matching the gRNA variable region and a protospacer adjacent motif (PAM) directly downstream of the target sequence.[10] It has been demonstrated that, although *Spy* CRISPR-Cas9 systems can cleave the intended target sequence with high efficiency, off-target cleavage occurs at DNA sequences that have base mismatches, deletions, or insertions relative to that of the gRNA.[13–20] Current strategies to reduce CRISPR-Cas9 off-target effects include the use of partially inactivated Cas9 nickases[21,22] and a catalytically dead Cas9 fused to the FokI endonuclease domain,[23–25] both of which require the design and delivery of two gRNAs. The requirement of a specific PAM sequence is quite strict, with *Spy* Cas9 recognizing NGG, and to a lesser extent NAG, and in rare instances other noncanonical sequences.[17] Although CRISPR-Cas9 systems from other species have also been studied,[26] apart from the *Staphylococcus aureus* (*Sau*) CRISPR-Cas9 system,[27] only very limited investigations have been made for their use to target endogenous loci in mammalian cells.[28]

The PAM sequence of a CRISPR system has important implications to its target specificity. Although base mismatches may be tolerated between the gRNA and targeted sequences, the PAM sequence has a stricter adherence to the consensus. This led to the hypothesis that an orthogonal CRISPR-Cas9 system with a longer PAM sequence may have fewer off-target cleavage events. Here, we report our studies of genome editing in mammalian cells using the CRISPR-Cas9 system from *Neisseria meningitidis (Nme)* that has previously been demonstrated to recognize a canonical PAM sequence NNNNGATT.[26,29,30] On average, the optimal PAM sequence (NGG) for the *Spy* CRISPR-Cas9 system is present once every eight bases in a random sequence when both sense and antisense orientations are taken into consideration, rising to once every 4 bp for all recognizable PAM sequences (NRG). In contrast, the optimal *Nme* Cas9 PAM sequence (NNNNGATT) occurs once every 128 bases in a random sequence, with the degenerate PAM NNNNGHTT occurring once every 96 bases, thus reducing the number of potential off-target sites. We show that compared with the *Spy* system, *Nme* systems exhibit a lower off-target effect at endogenous loci, while achieving similar or lower on-target

activities. Therefore, the *Nme* CRISPR-Cas9 system may represent a more specific alternative for precision genome engineering applications.

RESULTS

Determination of optimum guide RNA length

Previous studies of the *Nme* CRISPR-Cas9 systems used 24 and 20 nucleotides (nt) long gRNAs with 24 nt gRNAs more closely resembling the native length.[26,29,30] Since *Spy* Cas9 gRNAs with truncations were reported to have lower off-target activity,[31] we systematically tested *Nme* gRNAs ranging from 24 to 20 nt to determine the optimum gRNA length for high *Nme* Cas9 activity for both the native crRNA and tracrRNA system (2-RNA) where the crRNA and tracrRNA are separate and expressed from different U6 promoters, and a chimeric single guide RNA (sgRNA) system with crRNA and tracrRNA fused together and expressed from a single U6 promoter (**Figure 1a,b**). We found that the *Nme* CRISPR-Cas9 systems had non-homologous end joining-induced indel (small insertion and/or deletion) rates ranging from 3 to 75%. The levels of cleavage activity observed at each target locus varied based on the length of gRNA used (**Supplementary Table S1**). The 2-RNA system has a preference for a longer gRNA sequence (**Figure 1c,d**), whereas the sgRNA system seems to tolerate more variance in the length of the gRNA. Our results agree with a previous report that compared to T, nucleotide A is not favored as the first N base in the *Nme* PAM sequence (ANNNGATT).[29] We also observed lower activity when nucleotide T was the PAM proximal base of the target sequence (**Supplementary Figure S1**).

### Characterization of the dependence on protospacer-adjacent motif

The canonical PAM sequence for *Nme* Cas9 was bioinformatically determined to be NNNNGATT.[32] Similar to the *Spy* Cas9 that can recognize PAM sequences other than the canonical NGG motif, previous reports suggest that *Nme* Cas9 can also recognize non-canonical PAM sequences. However, these studies tested PAM recognition either in a bacteria cell[29] or with a limited number of possible PAMs.[30] To investigate the PAM preference of the *Nme* Cas9 system in mammalian cells, PAM sequences differing by one nucleotide at each position were tested in HEK293T cells to determine the effect on *Nme* CRISPR-Cas9 induced cleavage using a quantitative luciferase-based single-strand annealing (SSA) assay.[33] In this assay, two direct repeats of the firefly luciferase open reading frame are separated by a nuclease target site from *HPRT1* and two stop codons. Recognition and cleavage of the target site by a designer nuclease leads to repair of the DNA double-strand break via single-strand annealing between the two direct repeats, rescuing the expression of luciferase protein (**Figure 2a**). The use of this surrogate reporter system also removes any bias from site accessibility issues that may arise when targeting different endogenous loci. As expected, *Nme* Cas9 had high activity in the presence of the bioinformatically determined PAM sequence NNNNGATT. Consistent with previously reports, the NNNNGCTT and NNNNGTTT PAM sequences also facilitated high levels of *Nme* Cas9 activity.[26,29] Lower activities were observed with several other PAM sequences (**Figure 1e**). We found that the PAM motifs that facilitated *Nme* Cas9 activity

differed between the two gRNA conformations, with the 2-RNA *Nme* system displaying more variation in base recognition than the sgRNA *Nme* system (**Figure 1f**). Although the reduced activity of these novel PAM sequences precludes their use for targeted DNA cleavage, they should be considered when searching for potential off-target sites.

Comparison of targeting specificity between *Nme* Cas9 and *Spy* Cas9

Previous studies have shown that *Spy* CRISPR-Cas9 systems can tolerate genomic target sites containing base mismatches, single-base DNA insertions (DNA bulges) and single-base DNA deletions (RNA bulges),[13–16] which have significant implications to the targeting specificity of CRISPR-Cas9. To study the sequence mismatch tolerance of the *Nme* CRISPR-Cas9 system, we systematically modified single nucleotides at all positions throughout the *HPRT1* targeting gRNA (**Figure 2b**) and tested the ability of these gRNA variants to direct Cas9-mediated DNA cleavage by determining luciferase expression in an SSA based assay. The optimal gRNA length for each system was used and nucleotides at all positions were modified except the base at the 5′ end. This base must be a guanine as it is the transcription start site for the U6 promoter. Specifically, 23-base gRNAs were used for the 2-RNA *Nme* system, 21 bp gRNAs for the sgRNA *Nme* system, and 20bp gRNAs for the *Spy* system respectively. We found that the off-target cleavage due to single-base mismatches varied significantly among the three systems in a position-dependent fashion, with the *Spy* Cas9 system having a higher off-target effect at most of the locations when compared with the *Nme* Cas9 systems (**Figure 2b**, **Supplementary Table S2**).

To determine if the *Nme* CRISPR-Cas9 system could also tolerate target sites containing one-base DNA bulges, we systematically removed single nucleotides at all possible positions throughout the original *HPRT1*-targeting gRNAs for the three CRISPR-Cas9 systems (*spy*, 2-RNA *Nme*, and sgRNA *Nme*), resulting in gRNA-DNA interfaces containing one-base DNA bulges (**Figure 2d**, **Supplementary Table S2**). Luciferase-based SSA assays were used to determine CRISPR-Cas9-induced cleavage activity for each gRNA variant. We found that, similar to what we observed previously,[16] the *Spy* CRISPR-Cas9 system tolerated DNA bugles at the 5′ and 3′ ends, as well as at positions 10–14 nucleotides from the PAM site. The *Nme* CRISPR-Cas9 systems also showed DNA bulge tolerance, but with lower overall activity compared with the *Spy* system (**Figure 2d**). Specifically, the 2-RNA *Nme* system showed no DNA bulge tolerance in the central region, whereas the sgRNA *Nme* system displayed a significant level of activity with a DNA bulge at position 6/7/8. Note that this DNA bulge could also be modeled as having 3 mismatches at positions 1, 4, and 6, and a noncanonical PAM that is not recognized by *Nme* (NNNNTTTA) (**Supplementary Figure S2a**). Similarly, for the *Spy* system, certain DNA bugles may be interpreted as base mismatches. For example, removing the 5′-end bases (base 17, 18, or 19) results in a truncated gRNA with one or two base mismatches, and the 3′-end base deletions (base 1/2/3) results in a 19-nt gRNA with a shifted PAM sequence (GGG to AGG) (**Supplementary Figure S2b**), which may explain why the activity for the *Spy* Δ3/2/1 gRNA is similar to the original *HPRT1* gRNA.
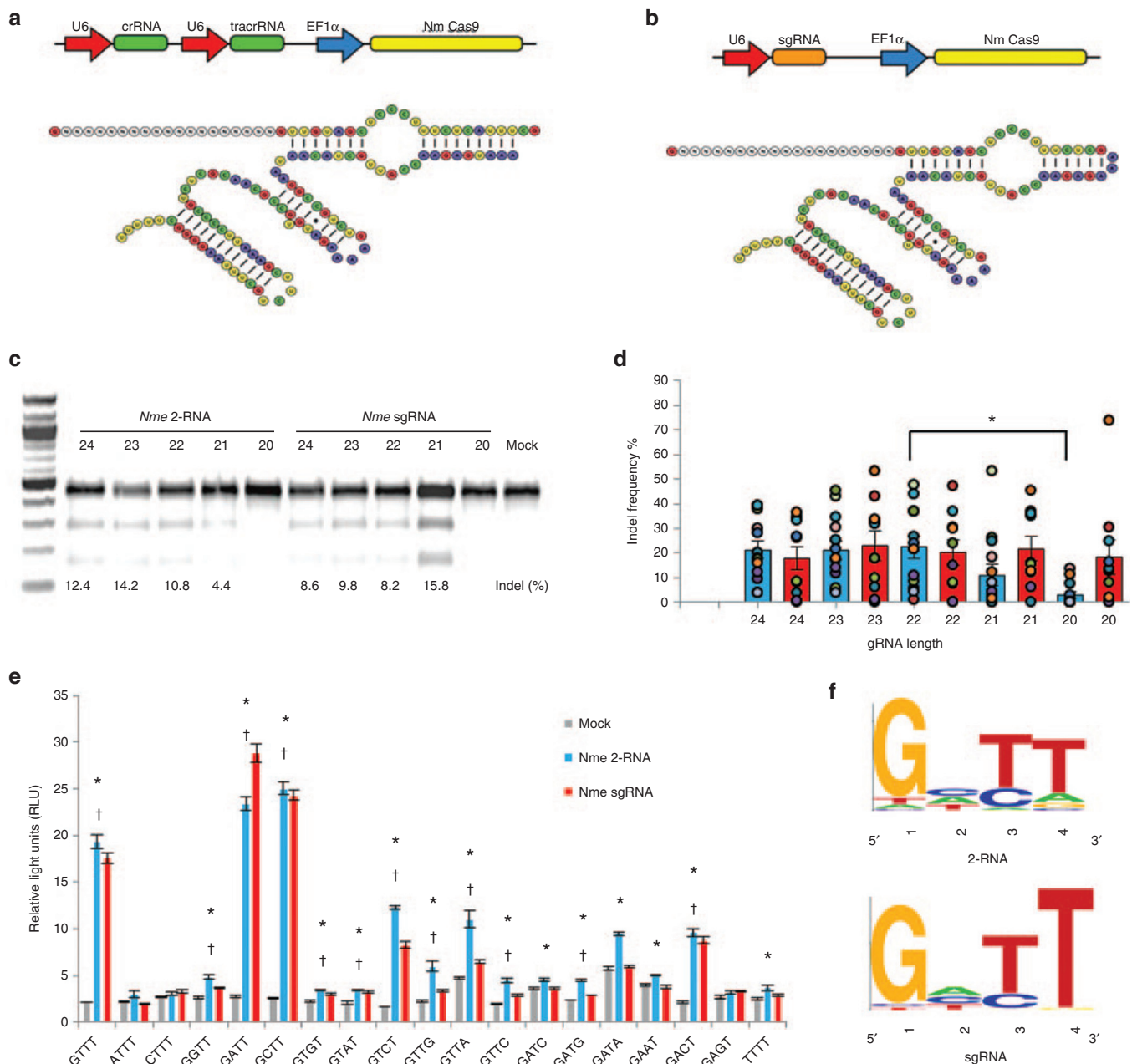
Figure 1 Overview of the *Nme* CRISPR-Cas9 system. Outline of the expression systems and the predicted structures of the of the 2-RNA **(a)** and sgRNA **(b)** systems. **(c)** T7EI assay showing activity of the *Nme* 2-RNA system and the *Nme* sgRNA system at the *IL2RG* locus in HEK 293T cells. **(d)** Activity of gRNAs with different lengths. Bars represent the average cutting efficiency for each length and the cutting activity for each locus tested is represented as circles. Data for the *Nme* 2-RNA system (blue bars) is taken from T7EI assay data from 13 endogenous loci and the data for the *Nme* sgRNA system (red bars) is taken from T7EI assay data from 10 endogenous loci. All experiments were carried out in HEK293T cells. gRNA lengths that had activity levels that differed significantly from the highest active gRNA length at denoted by *. Significance was determined using a two-tailed *t*-test. $P < 0.05$ **(e)** Luciferase single-strand annealing (SSA) assays to investigate protospacer adjacent motif (PAM) recognition of *Nme* Cas9. All data from biological triplicates. The significance of 2-RNA activity levels (*) and sgRNA activity levels (†) were determined using a two-tailed *t*-test. $P < 0.05$ **(f)** Extrapolated PAM sequence preference of the *Nme* CRISPR-Cas9 systems with 2-RNA (top) and the *Nme* sgRNA (bottom) based on results from Luciferase SSA assays.

However, off-target activities associated with centrally located DNA bulges (position 10–14) cannot be modeled as a result of base-mismatches.

To determine if *Nme* CRISPR-Cas9 systems could tolerate one-base RNA bulges, single nucleotides were added at each position throughout the original *HPRT1* gRNA sequences, resulting in

one-base RNA bugles at the gRNA-DNA interfaces. Inserted nucleotides differed from both flanking bases to ensure a single-base bulge at each position along the gRNA (**Supplementary Table S2**). The luciferase-based SSA assay was again used to determine the activity of all gRNA variants. Surprisingly, we found that for both the *Spy* and *Nme* sgRNA systems, RNA bulges outside the
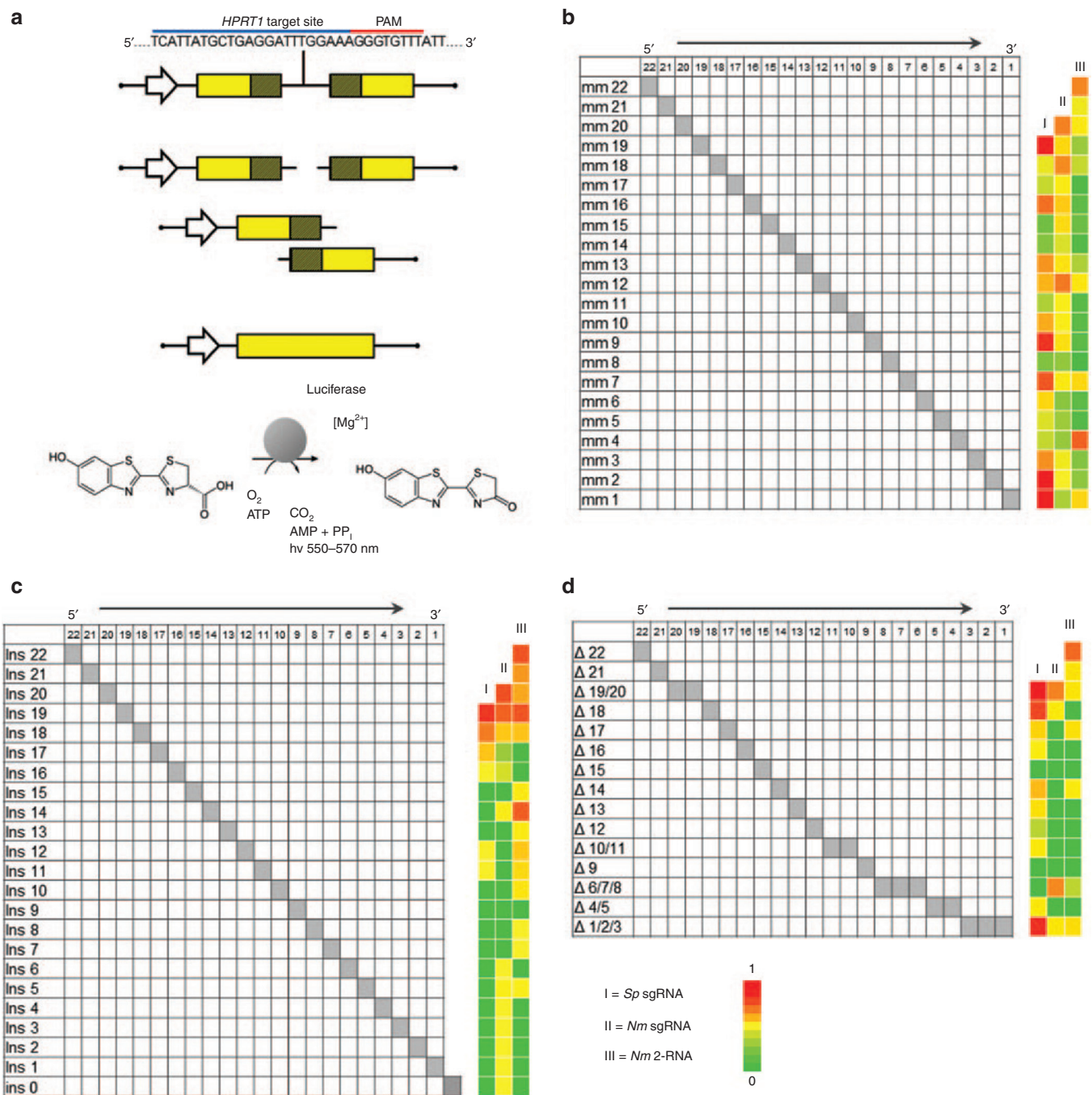
Figure 2 Comparison of mismatch tolerance between *Nme* and *Spy* CRISPR-Cas9 systems. (a) Schematic of the luciferase based single-strand annealing (SSA) assay used to determine gRNA specificity. Following successful cleavage of the target site by Cas9, the shaded homologous regions can recombine via SSA resulting in the restoration of the full length luciferase open reading frame and expression of luciferase. The level of luciferase expressed is measured by the amount of D-luciferin which is converted into oxyluciferin and light. The activity of gRNA variants containing mismatches **(b)**, insertions **(c)**, or deletions **(d)** are displayed as heatmaps based on relative single-strand annealing activity. The activity of all gRNA variants was normalized to the original guide sequence. gRNAs of 20, 21, and 23 nt were used for *Spy* sgRNA, *Nme* sgRNA, and *Nme* 2-RNA systems respectively. All data derived from biological triplicates. The sequences and raw data for all gRNA variants can be found in **Supplementary Table S3**.

5′ end abolished cleavage activity almost completely (**Figure 2c**). However, the *Nme* 2-RNA system with separate crRNA and tracrRNAs tolerated RNA bulges at the central region (position 10–15). These findings are similar to previously tested *Spy* gRNAs with similar GC contents.[16]

Comparison of *Nme* and *Spy* Cas9 on-target activity at overlapping endogenous loci

Direct comparison of the off-target profiles of *Nme* and *Spy* CRISPR/Cas9 systems at endogenous loci requires genomic sites with overlapping *Nme* and *Spy* PAM sequences and a shared
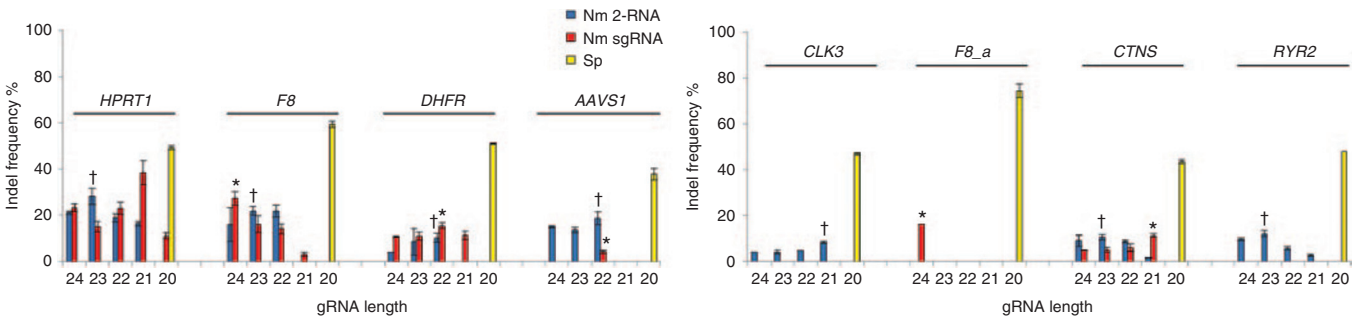
Figure 3 On-target activity of *Nme* and *Spy* CRISPR-Cas9 systems targeting endogenous loci in HEK293T cells. Both *Nme* and *Spy* gRNAs target overlapping protospacer sequences. Shown are cleavage activities of different CRISPR/Cas9 systems at eight genomic loci as measured using the T7EI assay. Data from biological replicates. For each locus both *Nme* Cas9 2-RNA and sgRNA gRNAs were compared to *Spy* Cas9. *Nme* 2-RNA gRNAs with significantly different values are denoted by † whereas *Nme* sgRNA gRNAs with significant differences in activity compared to *Spy* Cas9 are denoted by *. Statistical analysis was carried out for the gRNA length with the highest activity at each locus. *P* < 0.05.

Table 1 Number of potential off-target (OT) sites identified by COSMID

	F8			*DHFR*			*HPRT1*		
	≤ 3 mis.	Total	OT sites tested	≤ 3 mis.	Total	OT sites tested	≤ 3 mis.	Total	OT sites tested
Spy	61	259	20	146	613	20	188	721	19
Nme	3	17	17	5	24	20	17	44	19

Total number of sites includes sites with three or less mismatches, 1-bp insertion and up to two mismatches, and sites with 1-bp deletion and up to two mismatches in the first 19 protospacer adjacent motif proximal bases. The number of off-target sites investigated for each Cas9 ortholog targeting each gene is also listed.

protospacer sequence since it is widely accepted that different gRNAs may have different activity levels and off-target profiles. To identify shared overlapping *Spy* and *Nme* protospacers, genomic regions of interest were searched for the sequence NGGNGHTT containing the PAM sequence of *Nme* Cas9 (NNNNGHTT) and that of *Spy* Cas9 (NGG). In total, eight sites were selected with one site (*HPRT1*) containing the PAM sequence NGGNGTTT, and the other seven sites having the PAM sequence NGGNGATT. The activity of *Nme* and *Spy* CRISPR/Cas9 systems targeting these sites was assayed in HEK293T cells, with the activity levels determined using the T7EI assay. We found that the *Nme* systems targeting *HPRT1, F8*, and *DHFR* had activity levels as high as 40%, but were generally lower than that of *Spy* Cas9 (**Figure 3**). The cleavage activity of the *Nme* CRISPR/Cas9 systems at the remaining 5 target sites was substantially lower than that observed with the *Spy* system (**Figure 3**, **Supplementary Figure S3**).

The off-target activity profiles of *Nme* and *Spy* systems at overlapping endogenous loci

After comparing the ability of *Spy* and *Nme* CRISPR-Cas9 systems to tolerate single base mismatches, insertions, and deletions in a surrogate reporter system, we further investigated the off-target activity of *Spy* and *Nme* systems by determining if partially matched endogenous sequences are cleaved. Specifically, potential off-target sites for *Nme* and *Spy* gRNAs targeting *HPRT1, DHFR*, and *F8* were identified and ranked using the web-based tool COSMID.[34] For *Spy* gRNAs, sites with three or less base mismatches containing the NRG PAM were identified whereas for *Nme* gRNAs, sites with three base mismatches in the first 19 PAM proximal bases containing the NNNNGNTT PAM were identified. Sites with one base insertions and deletions were also identified for both the *Spy* and *Nme* systems. Overall, the number of

potential off-target sites identified for the *Nme* CRISPR-Cas9 systems was dramatically lower than that of the *Spy* system due to the requirement for a longer PAM sequence (**Table 1**). The top scoring off-target sites were amplified using locus-specific primers and sequenced using the Illumina Miseq platform. The on-target activity was also validated using deep sequencing for both the *Spy* and *Nme* systems. For each of the three target sites (*HPRT1, DHFR*, and *F8*), differences were observed in the mutation profiles between target loci. This is most likely due to differences in microhomology around the cleavage site[35] (**Supplementary Figure S4**). The measured indel rates at the sites tested for *Spy* are listed in **Table 2** while that for *Nme* are listed in **Table 3**. Interestingly, with the *Spy* CRISPR-Cas9 system, for each of the three target genes (*HPRT1, DHFR*, and *F8*), one off-target site was found to have a measurable level of cleavage activity (**Table 2**, **Figure 4**). In contrast, at all sites tested for the *Nme* CRISPR/Cas9 systems, no measurable off-target activities were detected (**Table 3**).

DISCUSSION

Unlike previous studies which targeted an integrated reporter system[28] or used an antibiotic selection system,[30] in this work, we directly determined the level of *Nme* Cas9 activity at endogenous loci in HEK293T cells. However, we found that the *Nme* Cas9 system has a larger variation in the on-target activity levels between target loci compared to that of the *Spy* system. This could be due to differences in the Cas9 proteins themselves, which differ in size by 287 amino acids. This difference in size could have an impact on several factors important for cleavage activity such as; site accessibility, binding stability, DNA unwinding and DNA cleavage. A recent report suggests that type II-C Cas9 orthologs, such as *Nme* Cas9 have poor DNA unwinding ability[36] which could account for the lower activity levels observed with *Nme* Cas9

Table 2 On- and off-target mutations and indel rates induced by *Spy* Cas9 designed to cleave endogenous genes

Target	Site name	Sequence	Indel rates		Closest gene	Feature
			Mock	Spy		
HPRT1	HPRT1	TTATGCTGAGGATTTGGAAAGGG	0.04	75.39	HPRT1	Exon
	SH_OT1	AGATGCTGAGGATTTGGAAACAG	0.02	13.87	ADAMTSL1	Intron
	SH_OT2	AAGTGCTGAGGATTTGGAAAAAG	0.02	0.03	FSCB	Intergenic
	SH_OT3	GTTTGTTGAGGATTTGGAAATAG	0.02	0.01	PTPRK	Intron
	SH_OT4	TGCTGGTGAGGATTTGGAAAAAG	0.12	0.08	GYPA	Intergenic
	SH_OT5	AGAGGGTGAGGATTTGGAAAGAG	0.02	0.01	PPP1R3F	Intron
	SH_OT6	ATCTGGCGAGGATTTGGAAAAAG	0.06	0.04	XACT	Intergenic
	SH_OT7	GTATTGAGAGGATTTGGAAAGAG	0.02	0.01	XPA	Intron
	SH_OT8	ATTTGCTGAAGATTTGGAAATGG	0.02	0.02	GPR19	Intergenic
	SH_OT9	ATAAGCTGAGGTTTTGGAAAGAG	0.03	0.03	LINC01488	Intergenic
	SH_OT10	TTATCCTGAGGCTTTGGAAAGAG	0.01	0.02	CWF19L2	Intergenic
	SH_OT11	AAATGCTTAGAATTTGGAAAAAG	0.04	0.04	LINC00331	Intergenic
	SH_OT12	CCAGGCTGAGCATTTGGAAACAG	0.01	0.02	EVA1A	Intron
	SH_OT13	TCATGCTCAGGGTTTGGAAAAAG	0.03	0.03	COL5A1	Intergenic
	SH_OT14	AGATACTGAGTATTTGGAAAGAG	0.02	0.02	LINC01515	Intergenic
	SH_OT15	CTCAGCTGAGGGTTTGGAAATGG	0.02	0.01	ZP3	Intron
	SH_OT16	TTCTTCTGAGTATTTGGAAAGAG	0.02	0.01	OR51B2	Intergenic
	SH_OT17	TTCTGCAGAGTATTTGGAAAAAG	0.06	0.04	MNX1	Intron
	SH_OT18	TTCTGCTTTGGATTTGGAAAGGG	0.03	0.03	BPESC1	Intron
	SH_OT19	TTTTGGTGAGGCTTTGGAAAGGG	0.03	0.04	PTPRD	Intergenic
DHFR	DHFR	TTTTATAGGTAAACAGAATCTGG	0.05	36.03	DHFR	Exon
	SD_OT1	TTTTATAGGTAAACAGAATCAAG	0.03	0.25	CDH4	Intron
	SD_OT2	AATTATTGGTAAACAGAATCCAG	0.01	0.01	ERICH6-AS1	Intron
	SD_OT3	AATTTTAGCTAAACAGAATCTGG	0.03	0.02	MIR5007	Intergenic
	SD_OT4	CTTTTGAGATAAACAGAATCTGG	0.07	0.04	CCNG1	Intergenic
	SD_OT5	CAATTTAGGTAAACAGAATCAAG	0.02	0.02	LINC01048	Intergenic
	SD_OT6	AAATACAGGTAAACAGAATCCAG	0.49	0.28	LOC101927847	Intergenic
	SD_OT7	AAATATTGGTAAACAGAATCCAG	0.01	0.00	SMC5	Intron
	SD_OT8	ATTTAGAAATAAACAGAATCCGG	0.02	0.01	SOX6	Intron
	SD_OT9	CTTTCTAGATAAACAGAATCAAG	0.06	0.03	LOC102723895	Intergenic
	SD_OT10	AATTACTGGTAAACAGAATCCAG	0.00	0.01	SLC22A25	Intron
	SD_OT11	GTTTTCAGGCAAACAGAATCTGG	0.02	0.03	TPM1	Intergenic
	SD_OT12	ATTATTATGTAAACAGAATCAAG	0.04	0.05	COBL	Intergenic
	SD_OT13	CCTAATAGTTAAACAGAATCCAG	0.00	0.01	LOC101928476	Intergenic
	SD_OT14	ATCTGTAGCTAAACAGAATCTAG	0.06	0.03	LPHN2	Intron
	SD_OT15	CTTTTTAGGAAAACAGAATCTAG	0.00	0.01	IL12A-AS1	Intron
	SD_OT16	TTTAATAGTGAAACAGAATCTGG	0.02	0.01	ARAP2	Intergenic
	SD_OT17	CTTAAGAGTTAAACAGAATCCAG	0.00	0.01	FJL33581	Intergenic
	SD_OT18	GTAGA-AGGTAAACAGAATCTGG	0.04	0.02	PSMA8 / DHFRP1	Intron
	SD_OT19	GTAGA-AGGTAAACAGAATCTGG	0.08	0.04	DHFRP2	Pseudogene
	SD_OT20	ATTATTAGGTCAACAGAATCTGG	0.01	0.01	FBN1	Intergenic
F8	F8	TCTAGTTGTGACAAGAACACTGG	0.04	54.95	F8	Exon
	SF_OT1	TGAAGTAGTGACAAGAACACTAG	0.03	0.02	RDH14	Intergenic
	SF_OT2	CCTCTATGTGACAAGAACACAAG	0.03	0.04	OR3A3	Intergenic
	SF_OT3	ACTTTGTGTGACAAGAACACTAG	0.01	0.02	LOC220729	Intergenic
	SF_OT4	CTTACTTTTGACAAGAACACTGG	0.03	0.02	CDH7	Intergenic
	SF_OT5	CCTGATTATGACAAGAACACTGG	0.01	0.01	TMEM39A	Intron
	SF_OT6	GCTATTTATAACAAGAACACGGG	0.01	0.04	LRP8	Intron
	SF_OT7	GCTAGCTGGTACAGAACACAGG	0.04	0.62	LINC01519	Intergenic
	SF_OT8	TTTAATTGTGATAAGAACACTAG	0.02	0.01	RBBP6	Intergenic
	SF_OT9	GCTGCTTGTGAGAAGAACACCAG	0.03	0.01	C14orf180	Intergenic
	SF_OT10	ACTAGATATGCCAAGAACACAAG	0.02	0.01	AMOTL1	Intergenic
	SF_OT11	CCTAGAGGTGAGAAGAACACAGG	0.03	0.01	TARID	Intron
	SF_OT12	CCTATTTCTGAAAAGAACACTAG	0.02	0.02	OR1A1	Intergenic
	SF_OT13	CTTAGTTGTCAGAAGAACACTGG	0.01	0.02	CD1D	Intergenic
	SF_OT14	ATTAGCTGTGACCAGAACACGAG	0.01	0.03	SLC2A13	Intergenic
	SF_OT15	AAT-GATGTGACAAGAACACAGG	0.04	0.02	LOC101927822	Intergenic
	SF_OT16	GCT-GATGTGACAAGAACACAAG	0.02	0.03	LOC339862	Intron
	SF_OT17	ACCTGT-GTGACAAGAACACTAG	0.01	0.02	RSPO2	Intron
	SF_OT18	AC-ATTAGTGACAAGAACACCAG	0.05	0.03	HDC	Intron
	SF_OT19	CCGAGTTGAGACTAGAACACAGG	0.01	0.02	KRT8	Intron
	SF_OT20	CCAAGTTGGGACCAGAACACAGG	0.03	0.03	LINC00877	Intergenic

Table 3 On- and off-target mutations and indel rates induced by *Nme* Cas9 designed to cleave endogenous genes

Target	Site name	Sequence	Mock	*Nme* sgRNA	Nme 2-RNA	Closest gene	Feature
HPRT1	HPRT1	ATCATTATGCTGAGGATTTGGAAAGGGTGTTT	0.04	24.01	33.06	*HPRT1*	Exon
	NH_OT1	CTTTTTGTGCTGTGGATTTGGAAACACTGTTT	0.01	0.02	0.01	*CDH12*	Intron
	NH_OT2	AGTTTTATGATGATGATTTGGAAAGAATGTTT	0.01	0.01	0.01	*MYH15*	Intron
	NH_OT3	TATCTTATGCAGAGGAATTGGAAAATGTGCTT	0.01	0.01	0.02	*TRPC6*	Intron
	NH_OT4	TACTTTCTGCAAAGGATTTGGAAAAACTGATT	0.02	0.02	0.02	*C2orf73*	Intron
	NH_OT5	CATATTTTGCTGCTGATTTGGAAAATGTGCTT	0.02	0.02	0.02	*ELAVL4*	Intron
	NH_OT6	CCCTTTAAGCTGGGCATTTGGAAAGGGAGGTT	0.03	0.02	0.02	*IL6R*	Exon
	NH_OT7	CAGCTTATGCTGAGGAAGTGGAAAGGTTGATT	0.01	0.01	0.01	*RELL1*	Intron
	NH_OT8	CATTTTATACTGAGGATATGGAAAGTGTGTTT	0.01	0.01	0.01	*HINT3*	Intergenic
	NH_OT9	CCCACTATGCAGAGGATTAGGAAAGGCTGATT	0.02	0.02	0.02	*HS6ST3*	Intergenic
	NH_OT10	TCATTTCTGCTGAGAATTTTGAAAGCACGTTT	0.01	0.02	0.01	*CDH2*	Intergenic
	NH_OT11	TAAATTATTCTGAGTATTTGAAAATAGAGTTT	0.01	0.01	0.02	*HMGN2P46*	Intergenic
	NH_OT12	CAAGATATGCTAAGGATTGGGAAAAGTGGCTT	0.02	0.03	0.02	*ZNF518B*	Intergenic
	NH_OT13	CAAGATATGCTAAGGATTGGGAAAAGTGGCTT	0.04	0.03	0.02	*ZNF518B*	Intergenic
	NH_OT14	TGTCTTGTGCTGGGGATTTGAAAAGTGGGGTT	0.01	0.01	0.01	*PDE1C*	Intron
	NH_OT15	CATATTCTGCTGAGGATCTGAAAAGTCTGCTT	0.00	0.04	0.00	*CYFIP1*	Intron
	NH_OT16	TGTATTACCCTGAGGATTTGGTAAGAGTGCTT	0.02	0.02	0.02	*MROH2A*	Intergenic
	NH_OT17	TTAATTATGTTGAGGATCTGGGAACTTTGATT	0.01	0.01	0.01	*TPBG*	Intergenic
	NH_OT18	ATGTTTATTCTGAGGATTTCGGAATATTGTTT	0.00	0.01	0.01	*STXBP5-AS1*	Intron
	NH_OT19	TTGACTATGCTGAGGATTTTGCAAATATGGTT	0.01	0.02	0.01	*PDZRN4*	Intergenic
DHFR	DHFR	GTGATTTTATAGGTAAACAGAATCTGGTGATT	0.05	11.55	19.73	*DHFR*	Exon
	ND_OT1	GAAATATTTCAGGTAAACAGAATCTCTTGTTT	0.00	0.00	0.00	*CYP7B1*	Intergenic
	ND_OT2	AAATTATTAT-GGGAAACAGAATCTGCAGATT	0.02	0.01	0.00	*NR3C2*	Intergenic
	ND_OT3	TTAATTTATTAGGTAAAAGAATCAAATGATT	0.07	0.11	0.07	*FOCAD*	Intron
	ND_OT4	TTTCTGTTTTAGG-AAACAGAATCTTCTGCTT	0.01	0.00	0.01	*VWDE*	Intergenic
	ND_OT5	TGTATTTTA-AGGGAAACAGAATCTGCAGTTT	0.01	0.01	0.00	*WDR86*	Intron
	ND_OT6	CTTGTTTTCTAGGTAA-CAGAATCTTATGTTT	0.01	0.02	0.02	*LYPLAL1*	Intergenic
	ND_OT7	TTTCTTTTAT-GGTAAAAATAATCATAAGATT	0.07	0.07	0.07	*CA10*	Intergenic
	ND_OT8	TTCTTTTTATAGGTTAA-AAAATCTAAAGATT	0.29	0.30	0.25	*PTCHD3*	Intergenic
	ND_OT9	AACTTTTTAAAGGTAAATA-AATCTGGGGTTT	0.06	0.05	0.03	*SIK3*	Intron
	ND_OT10	ATATTTTTATAGGGAAA-AGTATCCTTAGTTT	0.02	0.03	0.02	*MACF1*	Intron
	ND_OT11	CTCCTTTTGTAGG-AAACAGAAGCCTATGATT	0.01	0.02	0.01	*GPR158*	Intron
	ND_OT12	GATATTTTGAAGGTAAACAGAATATAGTGATT	0.01	0.00	0.00	*GRM8*	Intron
	ND_OT13	ATTGTTATACAGGTAAACAGAATTCTGAGTTT	0.02	0.02	0.01	*FOXG1-AS1*	Intergenic
	ND_OT14	GAAATTTTAGAG-TAAACAGAATTGAAGGATT	0.05	0.07	0.02	*CFTR*	Intergenic
	ND_OT15	TTATTTTTATAGGCAAACACATTCAAATGTTT	0.00	0.02	0.01	*LINC01432*	Intergenic
	ND_OT16	ACATTGTTAGAGGTAAACAGAAT-CCTTGTTT	0.01	0.02	0.01	*CADM2*	Intergenic
	ND_OT17	TCTTTTTTATTGGTAAA-AGAATAGACAGATT	0.02	0.02	0.02	*LOC388942*	Intergenic
	ND_OT18	AGAATTTTATTAGGTAAATAGAATATTAGGATT	0.01	0.01	0.01	*PRKG2*	Intron
	ND_OT19	TCATTTTTATAGTTAAAAGAAT-GATTGCTT	0.08	0.06	0.07	*ZWINT*	Intergenic
	ND_OT20	AAATTTTTATGGGTAAACAGTAT-ATGTGTTT	0.02	0.02	0.01	*ZNF277*	Intron
F8	F8	GGTTTCTAGTTGTGACAAGAACACTGGTGATT	0.04	29.28	27.63	*F8*	Exon
	NF_OT1	GTTATCAAGCTGTGAAAAGAACACTCTGGCTT	0.01	0.00	0.00	*LOC101928989*	Intergenic
	NF_OT2	CTCATCTTGTTGGGAC-AGAACACGGTTGATT	0.00	0.00	0.00	*PPP2R2C*	Intron
	NF_OT3	TCTGTCT-GTTGTCACTAGAACACATAAGCTT	0.02	0.01	0.01	*PPP1R13B*	Intron
	NF_OT4	CCATTCTAGATGTCACTAAGAACACTTGTGATT	0.01	0.01	0.02	*KCNC1*	Intron
	NF_OT5	GACTTCTAG-TGTGATTAGAACACCTCTGTTT	0.02	0.02	0.02	*L1TD1*	Intergenic
	NF_OT6	TGACTC-AGGTGTGACAACAACACTTCTGCTT	0.00	0.01	0.02	*KCNB2*	Intron
	NF_OT7	GAGATC-AGTGGTGACAATAACACATGTGATT	0.03	0.00	0.02	*OSBPL8*	Intergenic
	NF_OT8	CAATTCTACTTGTGAAAAAACACATTGGTTT	0.01	0.01	0.00	*TACR3*	Intron
	NF_OT9	TGCATTTAGTTG-GACAAAAACACCAAGGCTT	0.09	0.05	0.11	*PDHX*	Intron
	NF_OT10	CTGCTCT-GGTGTGACAAGACCACACATGATT	0.05	0.02	0.04	*HS3ST3B1*	Intergenic
	NF_OT11	AAGCTCTACTTGTAACAAGAA-ACTATGGTTT	0.01	0.01	0.01	*LPHN3*	Intron
	NF_OT12	TTATTTTA-TTGTGACAAGAACAGTTAAGTTT	0.00	0.01	0.02	*HTR2A*	Intergenic
	NF_OT13	TCCATCTAGTGGTCACAAGAACATCTCCAGATT	0.00	0.08	0.00	*COL23A1*	Intron
	NF_OT14	AACTTCTAGTTGTGGCAAGGA-ACACAGGTTT	0.06	0.01	0.03	*DPP9*	Intron
	NF_OT15	ATGCTCTAGTTCTGACA-GAACAGTCCTGATT	0.01	0.00	0.01	*NLGN1*	Intron
	NF_OT16	CCTGTCTACTTGTGACAA-AACAAATAGGCTT	0.00	0.01	0.03	*LINC00476*	Intergenic
	NF_OT17	GCTGACTAGTTGTGACAAGAACTATATGGTTT	0.01	0.01	0.02	*GRIA1*	Intron

Figure 4 Cleavage activity of *Spy* Cas9 at on- and off-target sites. Activity of *Spy* gRNAs targeting **(a)** *DHFR*, **(b)** *F8*, and **(c)** *HPRT1* at both on-target and off-target sites. **(d–f)** The target sequence at each locus is underlined and mismatches are highlighted in red. Sequence reads contain indels typical of non-homologous end joining repair following Cas9 cleavage. Only sites where activity levels were above 0.1% (as assessed by illumina MiSeq) are shown. Error bars represent 95% confidence intervals and *P* values were obtained using Fisher's exact test, *$P < 0.001$.

relative to *Spy* Cas9. *Nme* Cas9 also possesses DNase H activity which allows it to efficiently cleave ssDNA.[37] A deeper understanding of how the Cas9 nuclease interacts with both the gRNA and the DNA target may also shed some light on these differences. To this end, although the crystal structures of both *Spy* and *Sau* Cas9 proteins[38,39] have been determined, the crystal structure of *Nme* Cas9 protein has not yet been reported. We also observed differences in preference of gRNA length between the 2-RNA and sgRNA conformations. The sgRNA conformation used here was described previously.[29] This chimeric sgRNA has a shorter hybridization region between the tracrRNA and crRNA than the 2-RNA system and this could affect the stability of the *Nme* Cas9-gRNA ribonucleoprotein complex. The widely used *Spy* CRISPR-Cas9 sgRNA backbone sequence has been optimized to generate a highly active gene targeting system, suggesting that further modification of the *Nme* sgRNA may yield a more robust variant of the *Nme* CRISPR-Cas9 system with higher cleavage activity.

Interestingly, the effect of base mismatches, insertions (DNA bulges) and deletions (RNA bulges) on cleavage activity differed between *Nme* and *Spy* systems, and our results suggest that the *Nme* system has a lower tolerance to base mismatches and DNA bulges (**Figure 2b**, **Figure 2d**), leading to a better specificity. Here again, this difference in specificity could be a result of different Cas9 proteins and how they interact with both the gRNA and the DNA target.

Due to the longer PAM requirement of the *Nme* Cas9 system, for a specific genomic site to target, there are fewer partially matched sites present in the genome. Specifically, the NNNNGATT motif is expected to occur approximately once every 128 bp whereas the NGG motif recognized by *Spy* Cas9 occurs once every 8 bp. If all recognizable PAM sequences are considered, the *Spy* PAM NRG occurs once every 4 bp, whereas the *Nme* PAM NNNNGHTT occurs once every 96 bp. This lower prevalence of the *Nme* PAM allowed us to analyze all genomic sites containing at least three mismatches to the target sequence for the degenerate PAM NNNNGNTT. Encouragingly, we observed no activity at any site for three different *Nme* gRNAs in both the 2-RNA and sgRNA formats. Conversely, for each of three corresponding *Spy* gRNAs targeting the same endogenous loci we observed detectable levels of off-target activity ranging from 0.25 to 13.87%. This provides clear evidence that the *Nme* CRISPR-Cas9 system has a better specificity than that of the *Spy* system. Although having 4 N's in the *Nme* Cas9 PAM might provide an increased opportunity for non-specific interactions between the gRNA and the PAM, this should not result in increased off-target activity, since any interaction between the gRNA and the NNNN region of the PAM would likely result in low sequence homology between the remaining sequence of gRNA and target DNA, thus preventing Cas9 induced nonspecific cutting. Reduced off-target activity has recently been reported for other Cas9 orthologs with longer PAM sequences. For example, the off-target profile of *Sau* Cas9 was determined in three different studies.[27,40,41] In a direct comparison with *Spy* Cas9, *Sau* Cas9 was found to have less off-target effects.[27,41] Both the *Sth1* and *Sth3* orthologs were also shown to have lower off-target activity than *Spy* Cas9.[28]

Although all three *Spy* Cas9 gRNAs tested in this study had off-target activities, the off-target activity levels varied significantly. In general, different Cas9 gRNAs have different numbers of potential

off-target sites,[17] suggesting that the design of Cas9 gRNAs can be optimized. In particular, we note that all active off-target sites found in this study have a conserved seed region.[42–44] This region is necessary for DNA binding, and the seed region and PAM alone are sufficient for specific targeting by *Spy* Cas9.[44] Therefore, potential off-target sites containing mismatches in the seed region are less likely to result in Cas9 cleavage activity, and this can be used to select gRNAs with optimal activity and specificity. *In silico* search tools for off-target site identification may be employed to prescreen gRNAs to identify those with a low propensity for off-target cleavage, *i.e.*, gRNA with a low number of potential off-target sites and most (if not all) of these sites contain mismatches in the seed region.

Unlike *Spy* Cas9, the smaller size of the *Nme* Cas9 protein is within the packaging limit of AAV vectors which could be used for more efficient *in vivo* delivery for genome editing. Indeed, a recent study demonstrated that another small Cas9 ortholog, *Sau* Cas9 can be delivered efficiently *in vivo* using AAV.[27] The *Sau* Cas9 system also has a longer PAM sequence which differs slightly with that of *Nme* (NNGRRT). We believe that the characterization of the *Nme* system conducted in this study helps add a highly specific Cas9 ortholog to the CRISPR-Cas9 toolbox for a wide range of biological and medical applications.

MATERIALS AND METHODS

Construction of Nme CRISPR-Cas9 vector systems. The *Nme* Cas9 expressing plasmid pSimple-U6-tracr-U6-BsmBI-NLS-NMCas9-HA-NLS was a gift from Erik Sontheimer and James Thomson (Addgene plasmid #47868).[30] The region downstream of the U6 promoter driving crRNA expression was removed using BsmBI. Oligonucleotides containing partial crRNA sequence and two BsmBI sites for gRNA cloning were introduced to create pCL101. This modified cloning strategy requires only the 20–24 nucleotide (nt) guide sequence with appropriate BsmBI cloning overhangs to generate new gRNA constructs. Both U6 promoter regions were removed using AatII and BglII and a G-Block (IDT, Coralville, IA) containing a U6 promoter and a single gRNA (sgRNA) cassette with two BsmBI sites was cloned to create the *Nme* sgRNA vector pCL103. Both the 2-RNA system (pCL101) and the sgRNA system (pCL103) contain identical BsmBI overhang sequences facilitating simple cloning of new gRNA sequences into both systems using identical oligonucleotides.

CRISPR-Cas9 plasmid assembly. For *Nme* gRNAs, DNA oligonucleotides containing a G followed by a 19 to 23-nt guide sequence (**Supplementary Table S1**) were kinased, annealed, and ligated into both pCL101 and pCL103 plasmids. The annealed oligonucleotides have 4-bp overhangs that are compatible with the ends of BsmBI-digested pCL101 and pCL103 plasmids. For *Spy* gRNAs, DNA oligos containing a G followed by a 19-nt guide sequence were similarly kinased, annealed and ligated into BbsI digested pX330 (gift from Feng Zhang, Addgene plasmid #42230).[42] Constructed plasmids were sequenced to confirm the guide strand region using the primer CRISPR_Seq (5′-CGATACAAGGCTGTTAGAGAGATAATTGG-3′) for *Spy* and *Nme* sgRNA constructs or *Nme*2-RNA_Seq (5′-GGCGACACGGAAATG TTGAATACTC-3′) for *Nme* 2-RNA constructs.

T7 endonuclease I (T7EI) mutation detection assay for measuring endogenous gene modification rates. The cleavage activity of RNA-guided Cas9 at endogenous loci was quantified based on the mutation rates resulting from the imperfect repair of double-stranded breaks by non-homologous end joining. HEK293T cells were seeded 24 hours prior to transfection in 24-well plates at a density of 80,000 cells per well and cultured in Dulbecco's Modified Eagle Medium media supplemented with 10% fetal bovine serum and 2 mmol/l fresh L-glutamine. Cells were transfected

with 1,000 ng of Cas9_sgRNA plasmid using 2 μl of Lipofectamine 2000 (ThermoFisher Scientific, Grand Island, NY), according to manufacturer's instructions. Genomic DNA was harvested after 3 days using QuickExtract DNA extraction solution (Epicentre, Madison, WI). T7EI mutation detection assays were performed, as described previously[45] and the digestions separated on 2% agarose gels. The cleavage bands were quantified using ImageJ. The percentage of gene modification was determined using the formula, % non-homologous end joining = $100 \times (1 - (1 - \text{fraction cleaved})^{0.5})$, as described.[46] All polymerase chain reaction (PCR) reactions were performed using AccuPrime Taq DNA Polymerase High Fidelity (ThermoFisher Scientific, Grand Island, NY) following manufacturer's instructions for 40 cycles (94 °C, 30 seconds; 60 °C, 30 seconds; 68 °C, 45 seconds) in a 50 μl reaction containing 1 μl of the cell lysate, and 1 μl of each 10 μmol/l target region amplification primer (**Supplementary Table S1**).

Identification of off-target sites. Potential off-target sites in the human genome (hg19) were identified and ranked using the recently developed bioinformatics program COSMID,[34] allowing up to three base mismatches without insertions or deletions and two base mismatches with either an inserted or deleted base (bulge). The top ranked sites were further investigated. Primers used for target region amplification were designed by COSMID (**Supplementary Table S3**).

Luciferase-based single-strand annealing assay. For SSA assays, 10,000 cells were seeded per well in 96-well plates 24 hours prior to transfection. Each transfection contained 100 ng of DNA delivered using 0.4 μl of Lipofectamine 2000. Typically, transfections consisted of 25 ng of SSA target plasmid, 50 ng of CRISPR/Cas9 plasmid, 5 ng of Renilla luciferase plasmid and 20 ng of pUC18. Forty-eight hours post-transfection, luciferase expression was quantified using the Dual-Glo luciferase assay system (Promega, Madison, WI) and a Tecan (Mannedorf, Switzerland) Safire2 microplate reader. All SSA assays were carried out in triplicate.

Deep sequencing to quantify CRISPR-Cas9 activity at genomic loci. Genomic DNA from mock and nuclease-treated cells was amplified via PCR using locus-specific primers that contained adapter sequences for a second round of PCR (**Supplementary Table S3**). PCR reactions for each locus were performed independently for eight touchdown cycles in which annealing temperature was lowered by 1 °C each cycle from 65 to 57 °C, followed by 35 cycles with annealing temperature at 57 °C. PCR products were purified using Agencourt AmPure XP (Beckman Coulter) according to manufacturer's protocol. A second round of PCR amplification was performed for each individual amplicon using primers containing the adapter sequences from the first PCR, P5 and P7 adapters, and sample barcodes in the reverse primers. PCR products were purified as for first PCR, pooled in an equimolar ratio, and subjected to 2×250 paired-end sequencing on the Illumina MiSeq platform.

Paired-end reads from MiSeq were filtered by an average Phred quality (Qscore) greater than 20 and merged into a longer single read from each pair with a minimum overlap of 30 nucleotides using Fast Length Adjustment of SHort reads. Alignments to reference sequences were performed using Burrows-Wheeler Aligner for each barcode and percentage of insertions and deletions containing bases within a ±5-bp window of the predicted cut sites were quantified. Error bounds for indel percentages are Wilson score intervals calculated using binom package for R statistical software (version 3.0.3) with a confidence level of 95%. To determine if each off-target indel percentage from a CRISPR-treated sample is significant compared to a mock-treated sample, a two-tailed P value was calculated using Fisher's exact test.

SUPPLEMENTARY MATERIAL
Table S1. Activity of *Nm* gRNAs at different genomic loci.
Table S2. Luciferase SSA assay data.
Table S3. Activity of Sp and *Nm* CRISPR-Cas9 at predicted off-target loci.
Figure S1. Effect of sequence on *Nm* Cas9 activity.

Figure S2. Alternative modeling of DNA bulges as shorter gRNAs with alternate PAMs.

Figure S3. RepresentativeT7EI assay gel of CRISPR-Cas9 activity with gRNA lengths of 20 to 24 nt.

Figure S4. Indel profiles of different CRISPR-Cas9 systems.

REFERENCES
1. Barrangou, R, Fremaux, C, Deveau, H, Richards, M, Boyaval, P, Moineau, S *et al.* (2007). CRISPR provides acquired resistance against viruses in prokaryotes. *Science* **315**: 1709–1712.
2. Cho, SW, Kim, S, Kim, JM and Kim, JS (2013). Targeted genome engineering in human cells with the Cas9 RNA-guided endonuclease. *Nat Biotechnol* **31**: 230–232.
3. DiCarlo, JE, Norville, JE, Mali, P, Rios, X, Aach, J and Church, GM (2013). Genome engineering in Saccharomyces cerevisiae using CRISPR-Cas systems. *Nucleic Acids Res* **41**: 4336–4343.
4. Friedland, AE, Tzur, YB, Esvelt, KM, Colaiácovo, MP, Church, GM and Calarco, JA (2013). Heritable genome editing in C. elegans via a CRISPR-Cas9 system. *Nat Methods* **10**: 741–743.
5. Hwang, WY, Fu, Y, Reyon, D, Maeder, ML, Tsai, SQ, Sander, JD *et al.* (2013). Efficient genome editing in zebrafish using a CRISPR-Cas system. *Nat Biotechnol* **31**: 227–229.
6. Mali, P, Yang, L, Esvelt, KM, Aach, J, Guell, M, DiCarlo, JE *et al.* (2013). RNA-guided human genome engineering via Cas9. *Science* **339**: 823–826.
7. Shen, B, Zhang, J, Wu, H, Wang, J, Ma, K, Li, Z *et al.* (2013). Generation of gene-modified mice via Cas9/RNA-mediated gene targeting. *Cell Res* **23**: 720–723.
8. Wang, H, Yang, H, Shivalila, CS, Dawlaty, MM, Cheng, AW, Zhang, F *et al.* (2013). One-step generation of mice carrying mutations in multiple genes by CRISPR/Cas-mediated genome engineering. *Cell* **153**: 910–918.
9. Nekrasov, V, Staskawicz, B, Weigel, D, Jones, JD and Kamoun, S (2013). Targeted mutagenesis in the model plant Nicotiana benthamiana using Cas9 RNA-guided endonuclease. *Nat Biotechnol* **31**: 691–693.
10. Jinek, M, Chylinski, K, Fonfara, I, Hauer, M, Doudna, JA and Charpentier, E (2012). A programmable dual-RNA-guided DNA endonuclease in adaptive bacterial immunity. *Science* **337**: 816–821.
11. Urnov, FD, Miller, JC, Lee, YL, Beausejour, CM, Rock, JM, Augustus, S *et al.* (2005). Highly efficient endogenous human gene correction using designed zinc-finger nucleases. *Nature* **435**: 646–651.
12. Christian, M, Cermak, T, Doyle, EL, Schmidt, C, Zhang, F, Hummel, A *et al.* (2010). Targeting DNA double-strand breaks with TAL effector nucleases. *Genetics* **186**: 757–761.
13. Fu, Y, Foden, JA, Khayter, C, Maeder, ML, Reyon, D, Joung, JK *et al.* (2013). High-frequency off-target mutagenesis induced by CRISPR-Cas nucleases in human cells. *Nat Biotechnol* **31**: 822–826.
14. Hsu, PD, Scott, DA, Weinstein, JA, Ran, FA, Konermann, S, Agarwala, V *et al.* (2013). DNA targeting specificity of RNA-guided Cas9 nucleases. *Nat Biotechnol* **31**: 827–832.
15. Cradick, TJ, Fine, EJ, Antico, CJ and Bao, G (2013). CRISPR/Cas9 systems targeting β-globin and CCR5 genes have substantial off-target activity. *Nucleic Acids Res* **41**: 9584–9592.
16. Lin, Y, Cradick, TJ, Brown, MT, Deshmukh, H, Ranjan, P, Sarode, N *et al.* (2014). CRISPR/Cas9 systems have off-target activity with insertions or deletions between target DNA and guide RNA sequences. *Nucleic Acids Res* **42**: 7473–7485.
17. Tsai, SQ, Zheng, Z, Nguyen, NT, Liebers, M, Topkar, VV, Thapar, V *et al.* (2015). GUIDE-seq enables genome-wide profiling of off-target cleavage by CRISPR-Cas nucleases. *Nat Biotechnol* **33**: 187–197.
18. Frock, RL, Hu, J, Meyers, RM, Ho, YJ, Kii, E and Alt, FW (2015). Genome-wide detection of DNA double-stranded breaks induced by engineered nucleases. *Nat Biotechnol* **33**: 179–186.
19. Wang, X, Wang, Y, Wu, X, Wang, J, Wang, Y, Qiu, Z *et al.* (2015). Unbiased detection of off-target cleavage by CRISPR-Cas9 and TALENs using integrase-defective lentiviral vectors. *Nat Biotechnol* **33**: 175–178.
20. Kim, D, Bae, S, Park, J, Kim, E, Kim, S, Yu, HR *et al.* (2015). Digenome-seq: genome-wide profiling of CRISPR-Cas9 off-target effects in human cells. *Nat Methods* **12**: 237–43, 1 following 243.
21. Mali, P, Aach, J, Stranges, PB, Esvelt, KM, Moosburner, M, Kosuri, S *et al.* (2013). CAS9 transcriptional activators for target specificity screening and paired nickases for cooperative genome engineering. *Nat Biotechnol* **31**: 833–838.
22. Ran, FA, Hsu, PD, Lin, CY, Gootenberg, JS, Konermann, S, Trevino, AE *et al.* (2013). Double nicking by RNA-guided CRISPR Cas9 for enhanced genome editing specificity. *Cell* **154**: 1380–1389.
23. Guilinger, JP, Thompson, DB and Liu, DR (2014). Fusion of catalytically inactive Cas9 to FokI nuclease improves the specificity of genome modification. *Nat Biotechnol* **32**: 577–582.
24. Tsai, SQ, Wyvekens, N, Khayter, C, Foden, JA, Thapar, V, Reyon, D *et al.* (2014). Dimeric CRISPR RNA-guided FokI nucleases for highly specific genome editing. *Nat Biotechnol* **32**: 569–576.
25. Aouida, M, Eid, A, Ali, Z, Cradick, TJ, Lee, CM, Deshmukh, H *et al.* (2015). Efficient fdCas9 synthetic endonuclease with improved specificity for precise genome engineering. *PLoS One* **10**: e0133373 (doi: 10.1371/journal.pone.0133373).
26. Fonfara, I, Le Rhun, A, Chylinski, K, Makarova, KS, Lécrivain, AL, Bzdrenga, J *et al.* (2014). Phylogeny of Cas9 determines functional exchangeability of dual-RNA and Cas9 among orthologous type II CRISPR-Cas systems. *Nucleic Acids Res* **42**: 2577–2590.
27. Ran, FA, Cong, L, Yan, WX, Scott, DA, Gootenberg, JS, Kriz, AJ *et al.* (2015). *In vivo* genome editing using Staphylococcus aureus Cas9. *Nature* **520**: 186–191.
28. Müller, M, Lee, CM, Gasiunas, G, Davis, TH, Cradick, TJ, Siksnys, V *et al.* (2015). Streptococcus thermophilus CRISPR-Cas9 systems enable specific editing of the human genome. *Mol Ther* (epub ahead of print). doi: 10.1038/mt.2015.218.
29. Esvelt, KM, Mali, P, Braff, JL, Moosburner, M, Yaung, SJ and Church, GM (2013). Orthogonal Cas9 proteins for RNA-guided gene regulation and editing. *Nat Methods* **10**: 1116–1121.
30. Hou, Z, Zhang, Y, Propson, NE, Howden, SE, Chu, LF, Sontheimer, EJ *et al.* (2013). Efficient genome engineering in human pluripotent stem cells using Cas9 from Neisseria meningitidis. *Proc Natl Acad Sci USA* **110**: 15644–15649.
31. Fu, Y, Sander, JD, Reyon, D, Cascio, VM and Joung, JK (2014). Improving CRISPR-Cas nuclease specificity using truncated guide RNAs. *Nat Biotechnol* **32**: 279–284.
32. Zhang, Y, Heidrich, N, Ampattu, BJ, Gunderson, CW, Seifert, HS, Schoen, C *et al.* (2013). Processing-independent CRISPR RNAs limit natural transformation in Neisseria meningitidis. *Mol Cell* **50**: 488–503.
33. Cradick, TJ, Antico, CJ and Bao, G (2014). High-throughput cellular screening of engineered nuclease activity using the single-strand annealing assay and luciferase reporter. *Methods Mol Biol* **1114**: 339–352.
34. Cradick, TJ, Qiu, P, Lee, CM, Fine, EJ and Bao, G (2014). COSMID: A Web-based Tool for Identifying and Validating CRISPR/Cas Off-target Sites. *Mol Ther Nucleic Acids* **3**: e214.
35. Bae, S, Kweon, J, Kim, HS and Kim, JS (2014). Microhomology-based choice of Cas9 nuclease target sites. *Nat Methods* **11**: 705–706.
36. Ma, E, Harrington, LB, O'Connell, MR, Zhou, K and Doudna, JA (2015). Single-Stranded DNA Cleavage by Divergent CRISPR-Cas9 Enzymes. *Mol Cell* **60**: 398–407.
37. Zhang, Y, Rajan, R, Seifert, HS, Mondragón, A and Sontheimer, EJ (2015). DNase H Activity of Neisseria meningitidis Cas9. *Mol Cell* **60**: 242–255.
38. Nishimasu, H, Ran, FA, Hsu, PD, Konermann, S, Shehata, SI, Dohmae, N *et al.* (2014). Crystal structure of Cas9 in complex with guide RNA and target DNA. *Cell* **156**: 935–949.
39. Nishimasu, H, Cong, L, Yan, WX, Ran, FA, Zetsche, B, Li, Y *et al.* (2015). Crystal Structure of Staphylococcus aureus Cas9. *Cell* **162**: 1113–1126.
40. Kleinstiver, BP, Prew, MS, Tsai, SQ, Nguyen, NT, Topkar, VV, Zheng, Z *et al.* (2015). Broadening the targeting range of Staphylococcus aureus CRISPR-Cas9 by modifying PAM recognition. *Nat Biotechnol* **33**: 1293–1298.
41. Friedland, AE, Baral, R, Singhal, P, Loveluck, K, Shen, S, Sanchez, M *et al.* (2015). Characterization of Staphylococcus aureus Cas9: a smaller Cas9 for all-in-one adeno-associated virus delivery and paired nickase applications. *Genome Biol* **16**: 257.
42. Cong, L, Ran, FA, Cox, D, Lin, S, Barretto, R, Habib, N *et al.* (2013). Multiplex genome engineering using CRISPR/Cas systems. *Science* **339**: 819–823.
43. Jiang, W, Bikard, D, Cox, D, Zhang, F and Marraffini, LA (2013). RNA-guided editing of bacterial genomes using CRISPR-Cas systems. *Nat Biotechnol* **31**: 233–239.
44. Wu, X, Scott, DA, Kriz, AJ, Chiu, AC, Hsu, PD, Dadon, DB *et al.* (2014). Genome-wide binding of the CRISPR endonuclease Cas9 in mammalian cells. *Nat Biotechnol* **32**: 670–676.
45. Reyon, D, Tsai, SQ, Khayter, C, Foden, JA, Sander, JD and Joung, JK (2012). FLASH assembly of TALENs for high-throughput genome editing. *Nat Biotechnol* **30**: 460–465.
46. Guschin, DY, Waite, AJ, Katibah, GE, Miller, JC, Holmes, MC and Rebar, EJ (2010). A rapid and general assay for monitoring endogenous gene modification. *Methods Mol Biol* **649**: 247–256.